European Journal of Medicinal Chemistry 83 (2014) 155–166

Contents lists available at ScienceDirect

European Journal of Medicinal Chemistry

journal homepage: http://www.elsevier.com/locate/ejmech

Original article

Synthesis and antitumor activity of pyrido [2,3-*d*]pyrimidine and pyrido[2,3-*d*] [1,2,4]triazolo[4,3-*a*]pyrimidine derivatives that induce apoptosis through G_1 cell-cycle arrest

Mohamed Fares [a], Sahar Mahmoud Abou-Seri [b, *], Hatem A. Abdel-Aziz [c, d, **], Safinaz E.-S. Abbas [b], Mohieldin Magdy Youssef [e, f], Radwa Ahmed Eladwy [e]

[a] Department of Pharmaceutical Chemistry, College of Pharmacy, Egyptian Russian University, Badr City, Cairo, P.O. Box 11829, Egypt
[b] Department of Pharmaceutical Chemistry, Faculty of Pharmacy, Cairo University, Kasr El-Aini Street, Cairo, P.O. Box 11562, Egypt
[c] Department of Pharmaceutical Chemistry, College of Pharmacy, King Saud University, P.O. Box 2457, Riyadh 11451, Saudi Arabia
[d] Department of Applied Organic Chemistry, National Research Center, Dokki, Giza, P.O. Box 12622, Egypt
[e] Department of Pharmacology and Toxicology, College of Pharmacy, Egyptian Russian University, Badr City, Cairo, P.O. Box 11829, Egypt
[f] Department of Biology, School of Science and Engineering (SSE), American University in Cairo, New Cairo, P.O. Box 11835, Egypt

ARTICLE INFO

Article history:
Received 14 December 2013
Received in revised form
11 June 2014
Accepted 12 June 2014
Available online 13 June 2014

Keywords:
Pyrido[2,3-*d*]pyrimidine
Pyrido[2,3-*d*][1,2,4]triazolo[4,3-*a*]pyrimidine
Antitumor activity
Apoptosis
Cell cycle arrest

ABSTRACT

New series of 2-(2-arylidenehydrazinyl)pyrido[2,3-*d*]pyrimidines **5a**–**e** and pyrido[2,3-*d*][1,2,4]triazolo[4,3-*a*]pyrimidines **6**–**15** were synthesized and evaluated for their cytotoxic activity against two cancer cell lines, namely PC-3 prostate cancer and A-549 lung cancer. Some of the tested compounds displayed high growth inhibitory activity against PC-3 cells. Whereas, compounds **5b** and **15f** showed relatively potent antitumor activity against PC-3 and A-549 cell lines. In particular, 4-(3-acetyl-5-oxo-6-phenyl-8-(thiophen-2-yl)pyrido[2,3-*d*][1,2,4]triazolo[4,3-*a*]pyrimidin-1(5*H*)-yl)benzenesulfonamide **15f** exhibited superior antitumor activity against both cell lines at submicromolar level (IC_{50} = 0.36, 0.41 μM, respectively). Moreover, the potential mechanisms of the cytotoxic activity of the promising compound **15f** on the more sensitive cell line PC-3 were studied. The data indicated that **15f** was able to cause cell cycle arrest at least partly through enhancing the expression level of the cell cycle inhibitor p21 and induced cancer cell apoptosis via caspase-3 dependent pathway.

1. Introduction

Regardless of the immense advances in the field of basic and clinical research related to cancer therapy which have resulted in higher cure rates for a number of malignancies, cancer remains the second leading cause of death in developing as well as developed countries [1]. Chemotherapy is still one of the primary modalities for the treatment of cancer. However, the use of available chemotherapeutics is often limited mainly due to toxicities and drug-resistance [2]. This clearly underlies the urgent need of developing novel chemotherapeutic agents with safe potent antitumor activities.

Apoptosis or programmed cell death is a normal process that ensures equilibrium between cell proliferation and cell death and plays a regulatory role in controlling the size of cell populations as well as in tissues homeostasis [3]. Inadequate or abnormal inhibition of apoptosis leads to unchecked cell proliferation resulting in cell accumulation and is considered as a hallmark of cancer [4]. It has been reported that, drugs which restore the normal apoptotic pathway have the potential for effectively treating cancer that depend on aberration of apoptotic pathway to stay alive. This has encouraged a change in anticancer therapy trends, from classical cytotoxic strategies to the development of new non-harmful therapies which target apoptosis [5]. This process allows for the selective apoptotic destruction of oncogenic cells without causing vicinal inflammation in normal body tissues [6]. In addition, by inducing apoptosis, these new agents may overcome tumor resistance to conventional anticancer agents [7]. Therefore, the identification of apoptosis inducers has become an attractive approach for the discovery and development of potential anticancer agents.

* Corresponding author.
** Corresponding author. Department of Pharmaceutical Chemistry, College of Pharmacy, King Saud University, P.O. Box 2457, Riyadh 11451, Saudi Arabia.
E-mail addresses: saharshaarawy_69@yahoo.com (S.M. Abou-Seri), hatem_741@yahoo.com (H.A. Abdel-Aziz).

http://dx.doi.org/10.1016/j.ejmech.2014.06.027
0223-5234/

Among the wide range of compounds tested as potential anticancer agents, pyrido[2,3-*d*]pyrimidines were reported to exhibit antitumor activity which may be attributed to inhibition of cyclin dependent kinase [8,9], check point kinase [10] or mammalian target of rapamycin [11]. Moreover, several derivatives having pyrido[2,3-*d*]pyrimidine core were found to induce apoptosis and/or reduce cell proliferation in different solid tumors and leukemia cell lines [5,12–14]. For example, a series of 2,4-bis substituted pyrido[2,3-*d*]pyrimidines **I** exhibited dose dependent cytostatic effects against HT-29 colon cancer through activation of signaling pathways leading to cell cycle arrest and rapid apoptosis [5]. Later, 2-(alkylsulfanyl)-*N*-alkylarylpyrido[2,3-*d*]pyrimidine derivatives showed good profile as caspase-3 activator and apoptosis inducers in breast, colon and bladder cancer cells lines [12,13]. Furthermore, the novel analog; 2-[(3-chloro-4-fluorophenyl)amino]-6-(2,6-dichlorophenyl)-8-methylpyrido[2,3-*d*]pyrimidin-7(8*H*)-one **II** potently inhibited $p210^{Bcr\text{-}Abl}$ tyrosine kinase and induced apoptosis of K562 leukemic cell line [14].

On the other hand, several studies have been devoted to the antiproliferative activity of hydrazones, where a variety of hydrazone derivatives – like the hydrazinopyrimidines **III** – have been reported to inhibit the growth and/or induce apoptosis in a panel of human tumor cells including leukemia, lung, colon and breast cancer cell lines [15–17]. Stimulated by the successful applications of such class of compounds as apoptotic inducers, a new series of 2-(arylidenehydrazinyl)pyrido[2,3-*d*]pyrimidines **5a–e** was synthesized to explore the influence of incorporating hydrazonyl moiety on the antitumor activity of pyridopyrimidines (Scheme 1, Fig. 1).

Furthermore, 1,2,4-triazolo[4,3-*a*]pyrimidine ring system has been well acknowledged to possess anticancer activity [18–20]. This was exemplified by a series of triazolo[4,3-*a*]pyrimidin-6-sulfonamide derivatives **IV** that demonstrated potent inhibitory effects on the growth of a wide range of cancer cell lines including leukemia, prostate and lung cancer at low dose levels [18]. Accordingly, it seemed of interest to synthesize some fused pyrido[2,3-*d*][1,2,4]triazolo[4,3-*a*]pyrimidin-5-ones **6–15**, hoping that the hybridization of the pharmacophoric features of the triazolopyrimidine and pyridopyrimidine scaffolds would produce enhanced antitumor effect (Fig. 1). Surveying literatures revealed that no studies dealt with the anticancer activity of this tricyclic ring system concerning substitution at N-1 and C-3 positions. Therefore, structural modifications on pyrido[2,3-*d*][1,2,4]triazolo[4,3-*a*]pyrimidine core involved monosubstitution on the fused triazole ring with 3-oxo **7** or 3-amino **9** functionality as well as their isosteres 3-thioxo **8** and 3-methyl **10** derivatives (Scheme 2), in addition to 1,3-disubstitution as 3-acetyl-1-un/substituted phenyl **15a–e** and their ethyl carboxylate analogs **15g–j** (Scheme 3). The proposed structural modifications were aimed at gaining insight into the influence of some parameters like electronic nature, lipophilicity and steric effect on cytotoxic activity.

Herein, we report the synthesis, cytotoxic activity and structure activity relationship of new series of 2-(2-arylidenehydrazinyl) pyrido[2,3-*d*]pyrimidines **5a–e** and pyrido[2,3-*d*][1,2,4]triazolo[4,3-*a*]pyrimidines **6–15**. In addition, the most potent compound **15f** was selected to investigate its mechanism of action. Results showed that, it was able to cause cell cycle arrest and induced cancer cell apoptosis in PC-3 cell line via caspase-3 dependent pathway.

2. Results and discussion

2.1. Chemistry

The reaction between heterocyclic amines and aromatic α-β unsaturated ketones is a very convenient and versatile method for the fusion of the pyridine ring to the preexisting heterocycle [21]. The starting compound, 5-phenyl-7-(thiophen-2-yl)-2-thioxo-2,3-dihydropyrido[2,3-*d*]pyrimidin-4(1*H*)-one **3** was prepared via

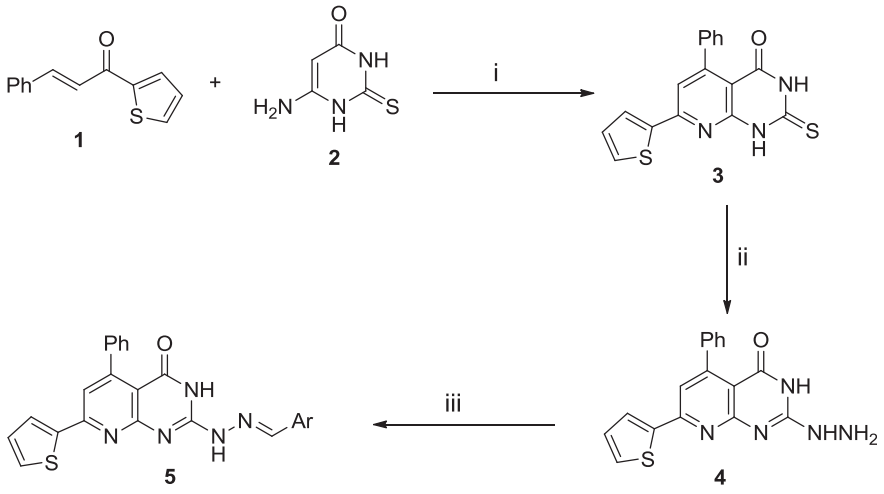

5	Ar
a	-C_6H_5
b	4-FC_6H_4
c	4-ClC_6H_4
d	4-MeC_6H_4
e	4-$MeOC_6H_4$

Scheme 1. Reagents and conditions: (i) dry DMF/reflux 15 h (yield: 70%); (ii) NH_2NH_2/absolute ethanol/reflux 15 h (yield: 70%); (iii) ArCHO/glacial acetic acid/reflux 4 h (yield: 88–92%).

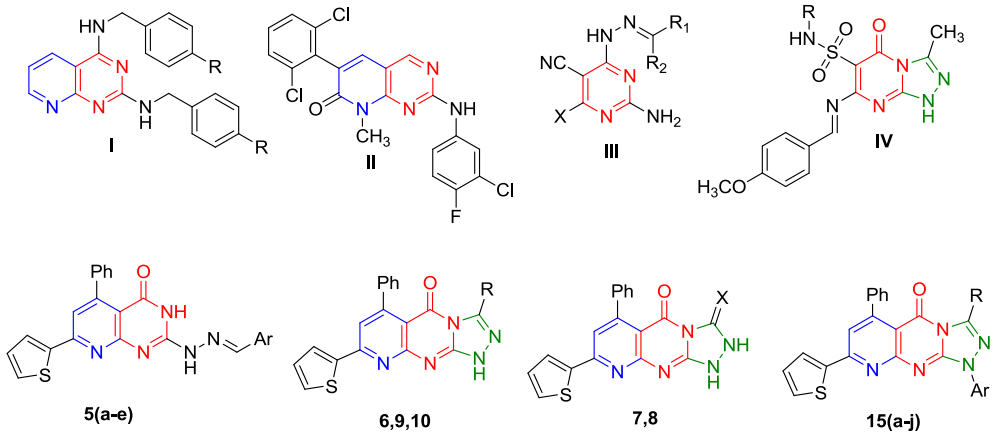

Fig. 1. Structure of some anticancer pyrido[2,3-*d*]pyrimidines **I,II**, hydrazinopyrimidines **III**, 1,2,4-triazolo[4,3-*a*]pyrimidines **IV** and the targeted compounds **5(a–e), 6–10** and **15(a–j)**.

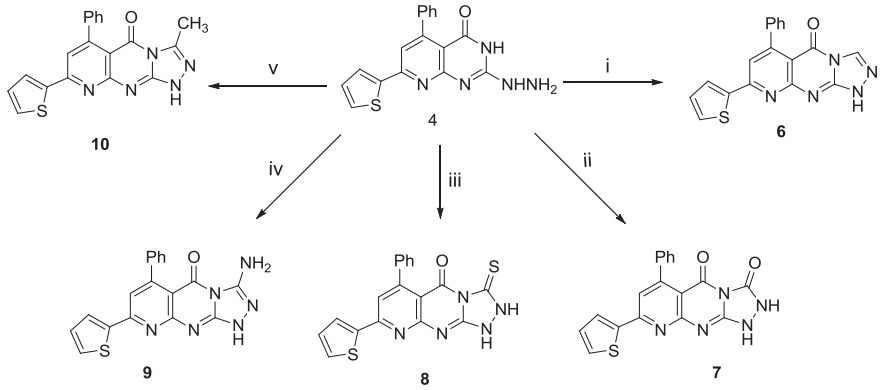

Scheme 2. Reagents and conditions: (i) triethyl orthoformate/reflux 3 h (yield: 72%); (ii) ethyl chloroformate/dry pyridine/reflux 9 h (yield: 86%); (iii) CS_2/KOH/absolute ethanol/reflux 5 h (yield: 62%); (iv) NH_4SCN/glacial acetic acid/reflux 10 h (yield: 68%); (v) acetyl chloride/dry pyridine/reflux 20 h (yield: 55%).

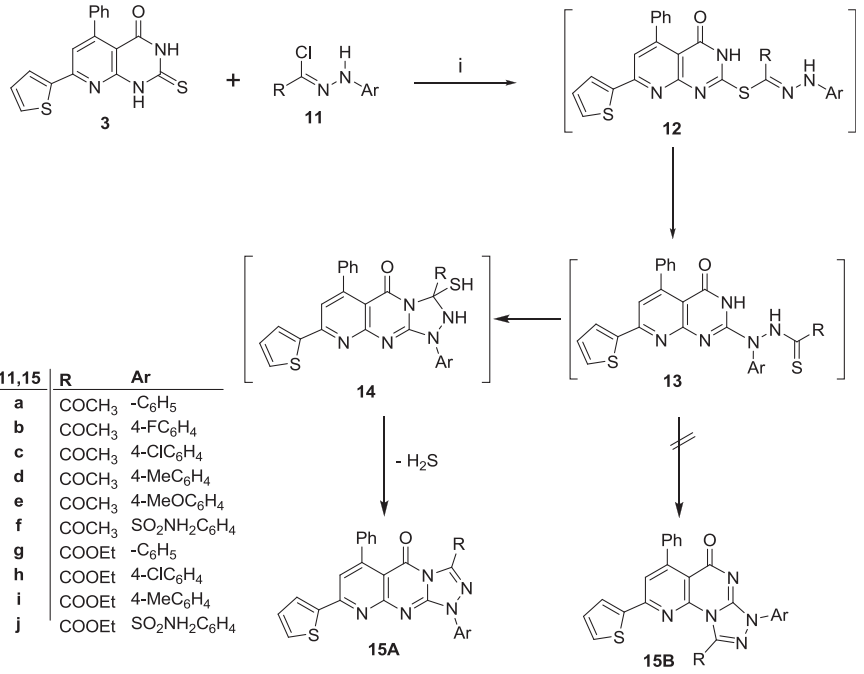

11,15	R	Ar
a	$COCH_3$	$-C_6H_5$
b	$COCH_3$	$4\text{-}FC_6H_4$
c	$COCH_3$	$4\text{-}ClC_6H_4$
d	$COCH_3$	$4\text{-}MeC_6H_4$
e	$COCH_3$	$4\text{-}MeOC_6H_4$
f	$COCH_3$	$SO_2NH_2C_6H_4$
g	COOEt	$-C_6H_5$
h	COOEt	$4\text{-}ClC_6H_4$
i	COOEt	$4\text{-}MeC_6H_4$
j	COOEt	$SO_2NH_2C_6H_4$

Scheme 3. Reagents and conditions: (i) TEA/dioxane/reflux 6–10 h (yield: 65–75%).

reacting 6-amino-2-thiouracil **2** and 3-phenyl-1-(thiophen-2-yl) prop-2-en-1-one **1** [22] in DMF according to the procedure reported by Quiroga et al. [23]. Reacting 2-thioxopyridopyrimidine **3** with hydrazine hydrate in absolute ethanol afforded 2-hydrazinylpyrido[2,3-*d*]pyrimidin-4(3*H*)-one **4**. Condensation of the latter with appropriate aldehyde furnished the required 2-(2-arylidenehydrazinyl)-5-phenyl-7-(thiophen-2-yl)pyrido[2,3-*d*]pyrimidin-4(3*H*)-ones **5a**–**e** (Scheme 1).

2-Hydrazinylpyrido[2,3-*d*]pyrimidin-4(3*H*)-one **4** is considered the key intermediate for the synthesis of a variety of 3-substituted pyrido[2,3-*d*][1,2,4]triazolo[4,3-*a*]pyrimidines **6**–**10**. Reacting the 2-hydrazinyl derivative **4** with triethyl orthoformate resulted in the formation of 6-phenyl-8-(thiophen-2-yl)pyrido[2,3-*d*][1,2,4]triazolo[4,3-*a*]pyrimidin-5(1*H*)-one **6**. While, cyclocondensation of the 2-hydrazinyl derivative **4** with ethyl chloroformate in dry pyridine or carbon disulphide in ethanolic KOH solution produced 3-oxo(thioxo)pyrido[2,3-*d*][1,2,4]triazolo[4,3-*a*]pyrimidines **7** and **8**, respectively. Alternatively, the 3-amino derivative **9** was obtained by refluxing the 2-hydrazinyl derivative **4** with ammonium isothiocyanate in acetic acid. Meanwhile, the preparation of the 3-methyl derivative **10** was achieved via the reaction of the 2-hydrazinyl derivative **4** with acetyl chloride in dry pyridine (Scheme 2).

Reaction of 2-thioxopyridopyrimidine **3** with hydrazonoyl chlorides **11a**–**j** in dioxane in the presence of triethylamine furnished one isolable product. As depicted in Scheme 3, the reaction proceeded through S-alkylation to give S-alkylated products **12** followed by Smiles rearrangement to afford intermediates **13** which were consumed in situ via elimination of hydrogen sulfide gas to give one of the isomeric fused triazole derivatives **15A** or **15B.** Both spectroscopic data (IR, ^{1}H NMR and Ms) and elemental analyses were consistent with either structure. The IR spectra of **15a**–**f** exhibited characteristic absorption band at 1710–1728 cm^{-1} due to acetyl C=O, while that of the ethyl carboxylate functionality in **15g**–**j** was observed at 1737–1755 cm^{-1}. ^{1}H NMR spectra of compounds **15a**–**f** displayed singlet signal resonating at δ 2.43–2.89 ppm representing acetyl CH_3 protons. Meanwhile, ^{1}H NMR of **15g**–**j** showed a typical triplet-quartet pattern of the ethyl protons at δ 1.30–1.31 and 4.42–4.44 ppm. Distinction between the two structures (**15A** or **15B)** was reached by comparing the ^{13}C NMR spectra with those of similar annulated pyrimidinones. Literature report [24] has shown that the chemical shift for the carbonyl carbon in pyrimidin-4-one derivatives is markedly affected by the nature of the adjacent nitrogen (pyrrole type as in **15A** or pyridine type as in **15B**). For example, ^{13}C NMR spectral data of compounds **15b** and **15f** revealed carbonyl carbon signals of the pyrimidinone at 162.44 and 162.62 ppm, respectively, suggesting that N-4 near to C=O is sp^3-hybridized (pyrrole type) which is different from C=O adjacent to a sp^2-hybridized nitrogen (pyridine type) that usually appears at 170–175 ppm [24]. Accordingly, the isolated products **15a**–**j** existed in one form namely, **A** rather than **B**. This result is in agreement with other reported cyclocondensation reactions of hydrazonoyl chloride with similar condensed 2-thioxopyridopyrimidine derivatives [25–27].

Furthermore, single-crystal X-ray analysis of compound **15g** gave an absolute confirmation for the structure of **15a**–**j,** in addition to a unique view for this system (Fig. 2). The X-ray analysis of compound **15g** showed the planarity of the tricyclic fused system as approximately planar system. It also revealed the presence of thiophene and phenyl of the 1,2,4-triazole in the same plane of the fused tricyclic system, while the phenyl ring on the pyridine is almost perpendicular to the main plane of the fused system. The X-ray analysis of compound **15g** displayed the binding resonance of ester function which is common in X-ray measurements at room temperature.

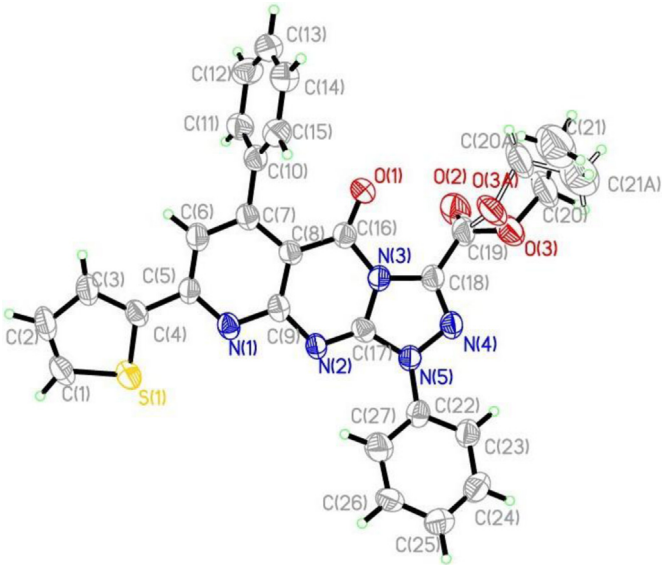

Fig. 2. ORTEP diagram of compound **15g**.

2.2. Biological activity

2.2.1. In vitro cytotoxic activity

Based on the reported cytotoxic activity of a large array of bioactive cores incorporating sulfonamide moiety, compound **15f** was selected to carry out a preliminary screening for its cytotoxic effects against four metastatic human cancer cell lines, including MCF-7 breast cancer, HepG2 liver cancer, A-549 lung cancer and PC-3 prostate cancer. The selection of such cell lines was inspired by the declared anticancer activity of a number of hydrazones, triazolo[4,3-*a*]pyrimidines and pyrido[2,3-*d*][1,2,4]triazolo[4,3-*a*]pyrimidine derivatives against the mentioned cell lines [15–18]. The cytotoxic activity was evaluated using the Sulfo-rhodamine B (SRB) colorimetric assay [28].The results revealed potent growth inhibitory activity against A-459 and PC-3 cell lines and fair activity against MCF-7 and HepG2 cancer cells (Table 1). Therefore, the cytotoxic activity of all the newly synthesized compounds was evaluated against the two sensitive cell lines, namely PC-3 and A-549. The conventional anticancer drug in clinical use, 5-fluorouracil was used as positive control. 5-FU is a pharmacologically nontoxic compound, which has been widely used in chemotherapy for a wide range of metastatic tumors including androgen-independent or hormone-refractory prostate cancer [29,30]. The cytotoxic activities are expressed as the median growth inhibitory concentration (IC_{50}) and are provided in Table 2. From the results, it is evident that some of the tested compounds displayed significant growth inhibitory activity. Compounds **5b, 5d** and **15f** (IC_{50} = 1.54, 0.63 and 0.36 μM, respectively) were found to be more potent and efficacious than 5-FU (IC_{50} = 12.00 μM) against PC-3 cell line. Moreover, compounds **6**, **7** and **9** were almost equipotent to the reference drug against the same cell line. In addition, compound **15f** was about 10

Table 1
Cytotoxic activity of compound **15f** against MCF-7, HepG2, A-549 and PC-3 cancer cell lines.

Compound	IC_{50} (μM)[a]			
	MCF-7	HepG2	A-549	PC-3
15f	37.96 ± 1.97	56.65 ± 3.65	0.41 ± 0.03	0.36 ± 0.02

[a] IC_{50} values are mean of three separate experiments ± S.D.

Table 2
Cytotoxic activity of the new compounds against A-549 and PC-3 cancer cell lines.

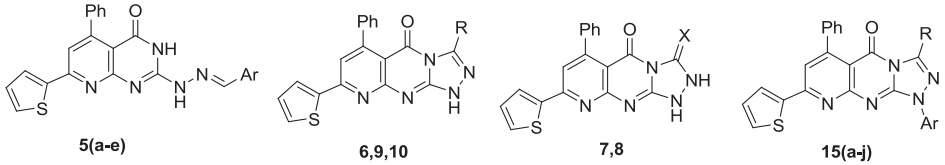

Compound	X	R	Ar	IC_{50} (μM)[a]	
				A-549	PC-3
5a	–	–	$-C_6H_5$	32.06 ± 3.41	26.80 ± 3.10
5b	–	–	$4\text{-}FC_6H_4$	3.36 ± 0.39	1.54 ± 0.19
5c	–	–	$4\text{-}ClC_6H_4$	40.75 ± 5.26	23.80 ± 2.46
5d	–	–	$4\text{-}MeC_6H_4$	56.60 ± 5.34	0.63 ± 0.07
5e	–	–	$4\text{-}MeOC_6H_4$	18.71 ± 0.61	18.22 ± 2.49
6	–	H	–	21.72 ± 2.54	11.71 ± 1.24
7	O	–	–	14.72 ± 1.76	12.66 ± 1.01
8	S	–	–	54.15 ± 3.76	32.39 ± 1.43
9	–	NH_2	–	43.73 ± 5.94	12.29 ± 0.99
10	–	CH_3	–	55.47 ± 6.70	83.88 ± 5.57
15a	–	$COCH_3$	C_6H_5	58.28 ± 4.80	32.33 ± 3.54
15b	–	$COCH_3$	$4\text{-}FC_6H_4$	39.05 ± 3.68	35.92 ± 3.85
15c	–	$COCH_3$	$4\text{-}ClC_6H_4$	30.56 ± 2.50	22.90 ± 1.5
15d	–	$COCH_3$	$4\text{-}MeC_6H_4$	19.33 ± 1.18	16.92 ± 1.54
15e	–	$COCH_3$	$4\text{-}MeOC_6H_4$	24.62 ± 2.65	19.47 ± 2.52
15f	–	$COCH_3$	$4\text{-}SO_2NH_2C_6H_4$	0.41 ± 0.03	0.36 ± 0.02
15g	–	$COOC_2H_5$	C_6H_5	26.64 ± 3.25	33.56 ± 2.21
15h	–	$COOC_2H_5$	$4\text{-}ClC_6H_4$	72.56 ± 7.45	37.43 ± 4.00
15i	–	$COOC_2H_5$	$4\text{-}MeC_6H_4$	37.80 ± 3.92	33.30 ± 2.74
15j	–	$COOC_2H_5$	$4\text{-}SO_2NH_2C_6H_4$	16.42 ± 1.69	7.15 ± 0.89
5-FU				4.21 ± 0.39	12.00 ± 1.15

[a] IC_{50} values are mean of three separate experiments ± S.D.

folds more potent than 5-FU against A-549 cell line (IC_{50} = 0.41, 4.21 μM, respectively), while compound **5b** (IC_{50} = 3.36 μM) exhibited slightly higher cytotoxic effect than that expressed by 5-FU.

Also, it was observed that PC-3 cell line was more susceptible to the influence of most of the tested compounds than A-549 cell line. With the exception of the sulfonamido derivative **15f** and 4-fluorobenzylidene derivative **5b**, the new compounds displayed poor antitumor activity against A-549 cell line, especially in comparison with 5-FU. Accordingly, the SAR of the target compounds will be discussed in relation to their activity toward PC-3 cell line. Analysis of the data in Table 2 showed that, 2-(2-arylidenehydrazinyl)pyridopyrimidines **5a**–**e** exhibited potent to moderate potency (IC_{50} = 0.63–26.80 μM). The highest growth inhibitory effect was associated with 4-methylbenzylidene **5d** and 4-fluorobenzylidene **5b** congeners (IC_{50} = 0.63, 1.54 μM, respectively), which displayed excellent activity relative to 5-FU (IC_{50} = 12.00 μM). Generally, the order of antitumor activity was found to be 4-methylbenzylidene **5d** > 4-fluorobenzylidene **5b** > 4-methoxybenzylidene **5e** > 4-chlorobenzylidene **5c** > unsubstituted benzylidene **5a**, indicating that substitution at the 4-position of benzylidene moiety with small electron donating (CH_3) or electron withdrawing (F) group of considerable lipophilicity greatly enhanced the activity (c.f. **5a**, **5b** and **5d**). Conversely, substitution with the more bulky chloro or methoxy substituent produced compounds with reduced cytotoxic activity, suggesting that the steric effect rather than the electronic nature of substituent may be the main factor affecting the potency of these compounds.

The pyrido[2,3-*d*][1,2,4]triazolo[4,3-*a*]pyrimidin-5-ones could be classified according to the substitution on the triazole ring into: 3-un/substituted 1,2,4-triazolo derivatives **6**–**10** and 1,3-disubstituted ones **15a**–**j**. Examination of the data concerning the 3-un/substituted derivatives **6**–**10** revealed that their anticancer activities were influenced by the C-3 substituent on the 1,2,4-triazole ring. The unsubstituted derivative **6** had potent growth inhibitory activity (IC_{50} = 11.71 μM) that is nearly equivalent to 5-FU (IC_{50} = 12.00 μM). Meanwhile, the 3-oxo derivative **7** and the 3-amino substituted counterpart **10** elicited similar cytotoxic activities (IC_{50} = 12.66 and 12.29 μM, respectively), which were however, slightly lower than the parent compound **6**, suggesting that substitution with a small hydrophilic group had little effect on potency. On the other hand, substitution with lipophilic group like the 3-thioxo derivative **8** and the 3-methylated analog **10** resulted in partial or complete loss of activity (IC_{50} = 32.39 and 83.88 μM, respectively).

Considering 1,3-disubstituted triazolo derivatives **15a**–**j**, the substituent on the N-1 phenyl ring appeared to be a determining factor for activity of 3-acetyl-1-un/substituted phenyl derivatives **15a**–**f** which exhibited a wide range of cytotoxic activity (IC_{50} = 0.36–35.95 μM). Compound **15a** having unsubstituted phenyl demonstrated fair cytotoxic effect (IC_{50} = 32.33 μM). Substitution on the phenyl ring with 4-fluoro resulted in compound **15b** with diminished activity (IC_{50} = 35.95 μM). Conversely, grafting 4-chloro, 4-methyl or 4-methoxy group to the phenyl ring contributed to an increase in potency (IC_{50} = 22.90, 16.92, 19.47 μM, respectively). Moreover, the introduction of 4-sulfonamido functionality afforded the most potent analog **15f** with superior antitumor activity (IC_{50} = 0.36 μM), highlighting the importance of sulfonamido substituent as a potential antitumor pharmacophore that is reported to play a vital role in the proper binding of several antitumor agents to their biotargets [31–33]. Finally, replacement of the 3-acetyl moiety in **15a, 15c, 15d** and **15f** with 3-ethyl carboxylate produced compounds **15g**–**j** with reduced cytotoxic efficacy, probably due to the low stability of ester function [34]. The

best growth inhibitory activity among the 3-ethyl carboxylate derivatives **15g–j** was observed with the benzenesulfonamide derivative **15j** (IC_{50} = 7.15 μM).

2.2.2. Morphological investigation

Chromatin condensation and fragmented nuclei are known as the classic characteristics of apoptosis [35]. Therefore, to determine whether the observed cell death induced by the most potent antiproliferative agent **15f** was due to apoptosis or necrosis, PC-3 treated cells were examined using acridine orange (AO) and ethidium bromide (EB) double staining under fluorescence microscopy after 24 h and 48 h of treatment [36].

AO permeates into living cells, emitting green fluorescence after intercalation into DNA. EB is only taken up by cells when cytoplasmic membrane integrity is lost, and stains the nucleus red. Thus live cells have normal green nuclei; early apoptotic cells have bright green nuclei and display condensed or fragmented chromatin; late apoptotic cells have orange stained nuclei with condensed and fragmented chromatin. Cells that have died from direct necrosis have a structurally normal red nucleus [37].

As shown in Fig. 3, it was found that the untreated control cells were morphologically normal, mostly green with intact nuclei (Fig. 3A). On the other hand, cells treated with **15f** at its IC_{50} displayed marked morphological changes. After 24 h of treatment, the cells were wrinkled, and the chromatin was condensed; some proportion of cells took only acridine orange and stained bright green with fragmented chromatin showing early apoptosis (Fig. 3B). While, after 48 h it was observed that yellow to orange fluorescence has been enhanced in some cells which indicated latter stage of apoptosis (Fig. 3C).

2.2.3. Caspase-3 activity (key executor of apoptosis)

It is well known that caspases, a family of proteolytic enzymes plays a pivotal role in the apoptotic process. Activation of these proteases – which are normally present inside cells as inactive zymogens – results in the cleavage of many protein substrates within the cell leading to irreversible apoptotic cell death. Among these caspases, caspase-3 is one of the most important downstream caspases and is called an effector caspase [38]. Therefore, the activation of caspase-3 in PC-3 cells treated with compound **15f** was investigated. The level of active caspase-3 was measured in ng/g protein using colorimetric assay that apply sandwich enzyme immunoassay technique. The assay uses monoclonal antibody and biotin conjugated antibodies, both of which are specific to caspase-3. As shown in Fig. 4, treatment of PC-3 cells with **15f** for 24 h and 48 h caused a significant increase in caspase-3 level by about 1.5 and 2 folds respectively, compared to control. These results supported the observation of chromatin condensation and DNA fragmentation during morphological investigations and suggested that **15f** induced apoptosis through activation of caspase-3.

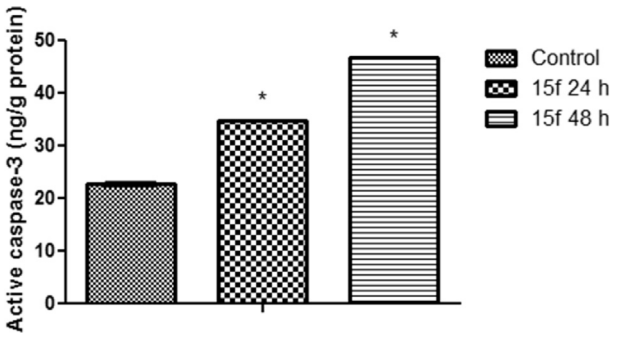

Fig. 4. Levels of active caspase-3 in PC-3 cells treated with IC_{50} of compound **15f** (0.36 μM) for 24 h and 48 h respectively. The experiment was done in triplicate. Data are mean ± SEM. *significantly different from control at $p < 0.05$.

2.2.4. Cell-cycle analysis

Cell cycle is the series of events that take place in a cell leading to its division and duplication (replication). The cell cycle consists of four distinct phases: G_1 phase, S phase (synthesis), G_2 phase (collectively known as interphase) and M phase (mitosis). During G1, preparation of energy and material for DNA replication occurs. The S phase is the stage when DNA replicates. During G_2, the new DNA is checked and any error is usually repaired. The M stage is "mitosis" when nuclear and cytoplasmic division occur [39].

The apoptosis inducing activity of **15f** was also characterized by flow cytometric analysis of the DNA profile in PC-3 cells. Fig. 5 showed that exposure of PC-3 cells to **15f** (0.36 μM) for 24 h induced a significant cell cycle arrest at G_0/G_1 phase with concurrent reduction in the percentage of cells at S and G_2/M phases compared to control. Meanwhile, exposure of PC-3 cells to **15f** for 48 h resulted in significant increase in the percentage of cells at the pre-G phase (cells with subdiploid DNA), a marker of apoptotic cells. These results were consistent with morphological observations and caspase-3 activation assay. The data also indicated that compound **15f** arrested cells in G_1 phase, with subsequent induction of apoptosis.

2.2.5. CDK4/Cyclin D1 and CDK6/Cyclin D1 profiling

Cyclin-dependent kinases (CDKs) are a family of protein kinases that is involved in regulating the cell cycle. They control the cell cycle progression from one phase to the next. Activation of CDKs is achieved via complexation with regulatory proteins called cyclins.

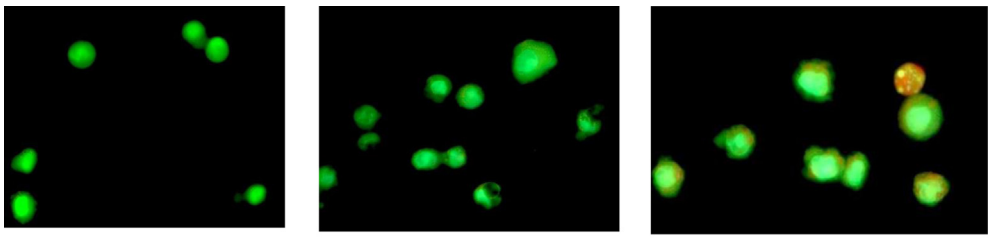

Fig. 3. Fluorescence photomicrographs of PC-3 cells stained using acridine orange/ethidium bromide (AO/EB). **(A)** Represents the control cells with intact nuclei stained uniformly green with AO. **(B)** and **(C)** show the apoptotic cells with chromatin condensation or nuclear fragmentation after treatment with compound **15f** at its IC_{50} for 24 h and 48 h respectively. The experiment was done in triplicate. (For interpretation of the references to color in this figure legend, the reader is referred to the web version of this article.)

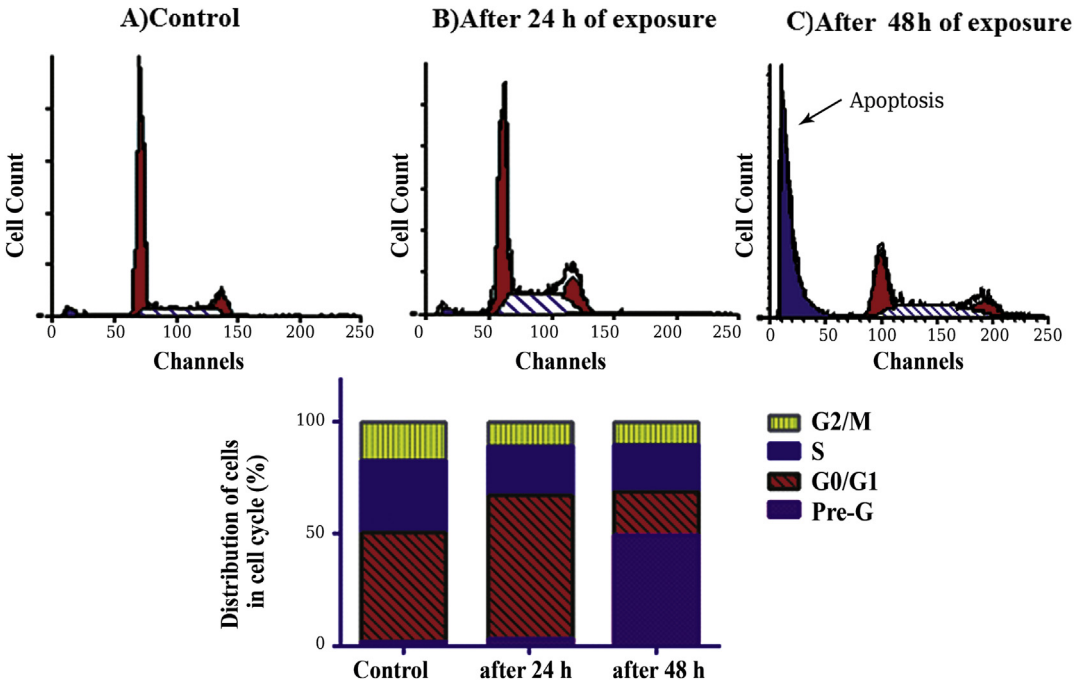

Fig. 5. DNA-flow cytometry analysis for PC-3 cells treated with compound **15f** for 24 h and 48 h at its IC_{50}. The experiment was done in triplicate. Data are mean ± SEM. *significantly different from control at $p < 0.05$.

Different types of cyclins and CDKs play their roles at various stages of the cell cycle. For instance, in the G_1 phase, CDK4 and CDK6 are activated upon binding with cyclin D1 leading to phosphorylation of the tumor suppressor protein retinoblastoma (pRb) [40]. Phosphorylation of Rb early in the G_1 phase indicates changes in gene transcription that carry cells through G_1/S transition and to DNA replication. Therefore, CDK4 or CDK6 inhibitors will inhibit Rb phosphorylation and prevent tumor cell from entering the S phase causing cell cycle arrest at G_1 phase resulting in suppression of DNA replication and decrease tumor cell proliferation [41].

To verify if the G_1 phase arrest caused by compound **15f** is mediated through CDK inhibition, the kinase inhibitory effect of **15f** was evaluated against CDK4 and CDK6 at concentrations of 1, 10 and 100 μM using radioisotope assay [42]. The broad spectrum CDK inhibitor staurosporine was used as a positive control. The profiling data in Table 3 showed that **15f** had weak inhibition at the highest tested concentration of the compound against both enzymes. At 100 μM, the CDK4/cyclin D1 and CDK6/cyclin D1 activities were inhibited by 21% and 17% respectively compared to control. On the other hand, staurosporine showed potent inhibition of both enzymes at 1 μM concentration, the CDK4/cyclin D1 and CDK6/cyclin D1 activities were inhibited by 93% and 90% respectively compared to control.

Table 3
The % inhibition of CDK4/Cyclin D1 and CDK6/Cyclin D1 in the presence of compound **15f** (1–100 μM) or staurosporine (1 μM).

Compound	Concentration	% inhibition	
		CDK4/Cyclin D1	CDK6/Cyclin D1
15f	1 μM	0	2
	10 μM	−5	−1
	100 μM	−21	−17
Staurosporine	1 μM	−93	−90

2.2.6. Expression levels of cyclin-dependent kinase inhibitor proteins p21 and p27

Cyclin-dependent kinase inhibitors p21 and p27 are proteins that bind to and inhibit the activity of CDK2/cyclin E, CDK4/cyclin D1 and/or CDK6/cyclin D1 complexes, and thus control the cell cycle progression at G1 phase [43]. The up regulated expression of these proteins is reported to mediate cell cycle G1 phase arrest in response to a variety of stress stimuli [44]. Therefore, the expression of p21 and p27 were examined in PC-3 cells treated with **15f** at IC_{50} (0.36 μM) by immunocytochemistry staining. Exposure to compound **15f** resulted in an elevation in the p21 positively stained PC-3 cells compared to control group (Fig. 6A). However, treatment with **15f** did not induce changes in the p27 expression in PC-3 cells (Fig. 6B). These results were further supported by Western blot analysis. The obtained data revealed that the protein level of p21 in PC-3 treated cells was increased by about 1.7 folds compared to control (Fig. 6C).

In summary, the sulfonamido derivative **15f** was able to cause G1 cell cycle arrest through enhancing the expression of cyclin-dependent kinase inhibitor p21 not by direct inhibition of CDK/cyclin activity.

3. Conclusion

New series of 2-(2-arylidenehydrazinyl)pyrido[2,3-*d*]pyrimidines **5a**–**e** and pyrido[2,3-*d*][1,2,4]triazolo[4,3-*a*]pyrimidines **6**–**15** were synthesized and evaluated for their cytotoxic activity against two cancer cell lines, namely PC-3 prostate cancer and A-549 lung cancer. The results revealed that compounds **5d, 6, 7** and **9** displayed high growth inhibitory activity against PC-3 cells. Whereas, compounds **5b** and **15f** showed relatively potent antitumor activity against both PC-3 and A-549 cell lines. In particular, 4-(3-acetyl-5-oxo-6-phenyl-8-(thiophen-2-yl)pyrido[2,3-*d*][1,2,4]triazolo[4,3-*a*]pyrimidin-1(5*H*)-yl)benzenesulfonamide **15f** exhibited superior antitumor activity against both cell

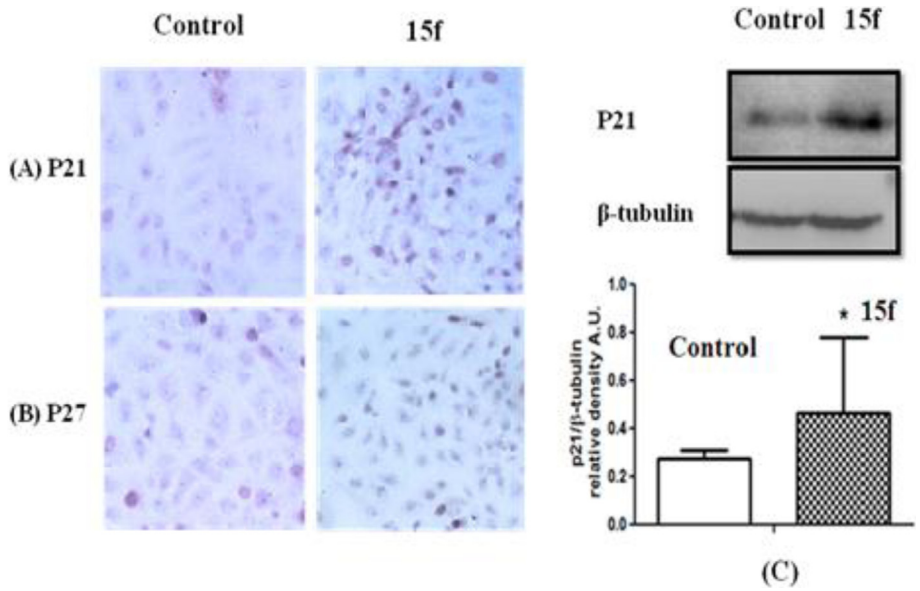

Fig. 6. Effect of compound **15f** on cell-cycle regulatory proteins in PC-3 cells treated with a fixed concentration (IC_{50}, 0.36 μM) of the tested compound for 48 h. (A) Immunocytochemistry staining for cyclin-dependent kinase inhibitor $p21^{CIP}$. (B) Immunocytochemistry staining for cyclin-dependent kinase inhibitor $p27^{kip}$. (C) Effect on the expression of p21 measured by Western blot. One of three repeated experiment is shown. * Significantly different from control at $P < 0.05$.

lines at submicromolar level (IC_{50} = 0.36, 0.41 μM, respectively). Moreover, the potential mechanisms of the cytotoxic activity of the promising compound **15f** on the more sensitive cell line PC-3 were investigated. The data indicated that **15f** was able to cause cell cycle arrest at least partly through boosting the expression level of the cell cycle inhibitor p21 as shown by immune-staining and western blotting. Also, **15f** exhibited pro-apoptotic activity as evidenced by its ability to induce nuclear fragmentation, in addition to augmenting caspase-3 activation. Hence, it could be considered as good lead-candidate for further optimization of new potent anti-tumor agents.

4. Experimental

4.1. Chemistry

4.1.1. General

Melting points were measured with a Gallenkamp apparatus and were uncorrected. IR spectra were recorded on Shimadzu FT-IR 8101 PC infrared spectrophotometer. The NMR spectra were recorded on a Bruker spectrophotometer at 300 or 400 MHz. ^1H NMR spectra were run at 300 or 400 MHz and ^{13}C NMR spectra were run at 75 or 100 MHz in deuterated dimethylsulphoxide (DMSO-d_6). Chemical shifts (δ_H) are reported relative to TMS as internal standard. All coupling constant (J) values are given in hertz. Chemical shifts (δ_C) are reported relative to DMSO-d_6 as internal standards. The abbreviations used are as follows: s, singlet; d, doublet; m, multiplet. Mass spectra were measured on a GCMS-QP1000 EX spectrometer at 70 e.V. Elemental analyses was carried out at the Regional Center for Microbiology and Biotechnology, Al-Azhar University, Cairo, Egypt and the results were within ±0.4%. Analytical thin layer chromatography (TLC) on silica gel plates containing UV indicator was routinely employed to follow the course of reactions and to check the purity of the products. All reagents and solvents were purified and dried by standard techniques.

4.1.2. 5-Phenyl-7-(thiophen-2-yl)-2-thioxo-2,3-dihydropyrido[2,3-d]pyrimidin-4(1H)-one (**3**)

A solution of 3-phenyl-1-(thiophen-2-yl) prop-2-en-1-one **1** (2.14 g, 0.01 mol) and 6-amino-2-thiouracil **2** (1.43 g, 0.01 mol) in dry DMF (30 mL) was refluxed for 15 h. The reaction mixture was cooled and the solid formed was filtered, dried and crystallized from DMF. Yield: 70%, m.p. > 300 °C; IR (KBr) ν: 3402 (NH), 1705 (C=O) cm^{-1}; ^1H NMR (DMSO-d_6, 300 MHz) δ: 7.18 (m, 1H, H^4 thiophene), 7.38–7.52 (m, 5H, Ar–H), 7.59 (m, 1H, H^5 thiophene), 7.92 (s, 1H, pyridine H), 8.07 (m, 1H, H^3 thiophene), 12.29 (br.s, 1H, NH, D_2O exchangeable), 13.05 (br.s, 1H, NH, D_2O exchangeable); MS m/z [%]: 339 [$(M+2)^+$, 23.70], 337 [M^+, 63.38], 83.05 [100]; Anal. Calcd $C_{17}H_{11}N_3OS_2$: C, 60.51; H, 3.29; N, 12.45; S, 19.01. Found: C, 60.30; H, 3.26; N, 12.59; S, 19.08.

4.1.3. 2-Hydrazinyl-5-phenyl-7-(thiophen-2-yl)pyrido[2,3-d]pyrimidin-4(3H)-one (**4**)

A mixture of 2-thioxopyrido[2,3-*d*]pyrimidine **3** (1.36 g, 4 mmol) and hydrazine hydrate (3 mL, 99%, 60 mmol) in absolute ethanol (20 mL) was heated under reflux for 15 h. The reaction mixture was cooled and the solid formed was filtered, dried and crystallized from DMF. Yield: 70%; m.p. 285–290 °C; IR (KBr) ν: 3317, 3336 (NH, NH_2), 1681 (C=O) cm^{-1}; ^1H NMR (DMSO-d_6, 300 MHz) δ 5.22 (br.s, 2H, $NH\underline{NH_2}$, D_2O exchangeable), 7.16 (m, 1H, H^4 thiophene), 7.38–7.42 (m, 5H, Ar–H), 7.59 (s, 1H, pyridine H), 7.62 (m, 1H, H^5 thiophene), 7.96 (m, 1H, H^3 thiophene), 8.25 (br.s, 1H, $\underline{NH}NH_2$, D_2O exchangeable), 12.15 (br s, 1H, NH pyrimidine, D_2O exchangeable); MS m/z [%]: 337 [$(M+2)^+$, 83.58], 335 [M^+, 14.08], 304 [100]. Anal. Calcd for $C_{17}H_{13}N_5OS$: C, 60.88; H, 3.91; N, 20.88. Found: C, 60.92; H, 3.97; N, 21.04.

4.1.4. 2-(2-Arylidenehydrazinyl)-5-phenyl-7-(thiophen-2-yl)pyrido[2,3-d]pyrimidin-4(3H)-ones ***5a–e***

A mixture of 2-hydrazinylpyrido[2,3-*d*]pyrimidine **4** (0.34 g, 1 mmol) and the appropriate aldehyde (benzaldehyde, 4-fluorobenzaldehyde, 4-chlorobenzaldehyde, 4-tolylaldehyde or 4-anisaldehyde) (2 mmol) in glacial acetic acid (15 mL) was heated

under reflux for 4 h. The reaction mixture was cooled and the solid formed was filtered, dried and crystallized from DMF/Ethanol [v:v, 1:1].

*4.1.4.1. 2-(2-Benzylidenehydrazinyl)-5-phenyl-7-(thiophen-2-yl)pyrido[2,3-d]pyrimidin-4(3H)-one (**5a**).* Yield: 92%; m.p. 293–295 °C; IR (KBr) ν: 3365 (NH), 1647 (C=O) cm^{-1}; ^1H NMR (DMSO-d_6, 300 MHz) δ: 7.21 (m, 1H, H^4 thiophene), 7.40–7.45 (m,9H, 8 Ar–H + pyridine H), 7.77 (m, 1H, H^5 thiophene), 7.95–8.03 (m, 3H, 2 Ar–H + H^3 thiophene), 8.12 (s, 1H, –N=CH), 11.29 (s, 1H, –NH–N=, D_2O exchangeable), 11.89 (s, 1H, NH pyrimidine, D_2O exchangeable); MS *m/z* [%]: 425 [$(M+2)^+$, 7.84], 423 [M^+, 92.08], 346 [100]. Anal. Calcd for $C_{24}H_{17}N_5OS$: C, 68.07; H, 4.05; N, 16.54. Found: C, 68.14; H, 4.11; N, 16.73.

*4.1.4.2. 2-(2-(4-Fluorobenzylidene)hydrazinyl)-5-phenyl-7-(thiophen-2-yl)pyrido[2,3-d]pyrimidin-4(3H)-one (**5b**).* Yield: 88%; m.p. > 300 °C; IR (KBr) ν: 3381 (NH), 1645 (C=O) cm^{-1}; ^1H NMR (DMSO-d_6, 300 MHz) δ: 7.18–7.28 (m, 3H, H^4 thiophene, 2 Ar–H), 7.42–7.45 (m, 6H, 5 Ar–H + pyridine H), 7.77 (m, 1H, H^5 thiophene), 8.03–8.1 (m, 3H, 2 Ar–H + H^3 thiophene), 8.12 (s, 1H, –N=CH), 11.37 (s, 1H, –NH–N=, D_2O exchangeable), 11.87 (s, 1H, NH pyrimidine, D_2O exchangeable); ^{13}C NMR (DMSO-d_6, 100 MHz) δ: 115.82, 116.04, 116.26, 127.82, 128.16, 128.36, 128.94, 129.19, 130.22, 130.30, 131.18, 131.59, 140.03, 144.29, 151.65, 153.75, 161.22, 162.18, 164.64, 172.50. MS *m/z* [%]: 443 [$(M+2)^+$, 7.84], 441 [M^+, 92.08], 346 [100]. Anal. Calcd for $C_{24}H_{16}FN_5OS$: C, 65.29; H, 3.65; N, 15.86. Found: C, 65.32; H, 3.71; N: 16.02.

*4.1.4.3. (2-(4-Chlorobenzylidene)hydrazinyl)-5-phenyl-7-(thiophen-2-yl)pyrido[2,3-d]pyrimidin-4(3H)-one (**5c**).* Yield: 90%; m.p. > 300 °C; IR (KBr) ν: 3381 (NH), 1658 (C=O) cm^{-1}; ^1H NMR (DMSO-d_6, 300 MHz) δ: 7.19 (m, 1H, H^4 thiophene), 7.42–7.51 (m, 8H, 7 Ar–H + pyridine H), 7.72 (m, 1H, H^5 thiophene), 7.89–7.92 (m, 3H, 2 Ar–H + H^3 thiophene), 8.08 (s, 1H, –N=CH), 11.40 (s, 1H, –NH–N=, D_2O exchangeable), 11.85 (s, 1H, NH pyrimidine, D_2O exchangeable); MS *m/z* [%]: 459 [$(M+2)^+$, 24], 457 [M^+, 72.45], 171 [100]. Anal. Calcd for $C_{24}H_{16}ClN_5OS$: C, 62.95; H, 3.52; N, 15.29. Found: C, 62.97; H, 3.57; N: 15.36.

*4.1.4.4. 2-(2-(4-Methylbenzylidene)hydrazinyl)-5-phenyl-7-(thiophen-2-yl)pyrido[2,3-d]pyrimidin-4(3H)-one (**5d**).* Yield: 90%; m.p. > 300 °C; IR (KBr) ν: 3427 (NH), 1728 (C=O) cm^{-1}; ^1H NMR (DMSO-d_6, 300 MHz) δ: 2.34 (s, 3H, CH_3), 7.18–7.24 (m, 3H, H^4 thiophene + 2 Ar–H), 7.43–7.49 (m, 6H, 5 Ar–H + pyridine H), 7.76 (m, 1H, H^5 thiophene), 7.84 (d, J = 7.8 Hz, 2H, Ar–H), 8.01 (m, 1H, H^3 thiophene), 8.08 (s, 1H, –N=CH), 11.21 (s, 1H, –NH–N=, D_2O exchangeable), 11.76(s, 1H, NH pyrimidine, D_2O exchangeable); MS *m/z* [%]: 439 [$(M+2)^+$, 8.72], 437 [M^+, 100]. Anal. Calcd for $C_{25}H_{19}N_5OS$: C, 68.63; H, 4.38; N, 16.01. Found: C, 68.67; H, 4.41; N: 16.14.

*4.1.4.5. 2-(2-(4-Methoxybenzylidene)hydrazinyl)-5-phenyl-7-(thiophen-2-yl)pyrido[2,3-d] pyrimidin-4(3H)-one (**5e**).* Yield: 89%; m.p. 298–300 °C; IR (KBr) ν 3385 (NH), 1676 (C=O) cm^{-1}; ^1H NMR (DMSO-d_6, 300 MHz) δ: 3.82 (s, 3H, OCH_3), 6.98 (d, J = 9 Hz, 2H, Ar–H),7.20 (m, 1H, H^4 thiophene), 7.42 (m, 6H, 5 Ar–H + pyridine H), 7.77 (m, 1H, H^5 thiophene), 7.88 (d, J = 9 Hz, 2H, Ar–H), 8.01 (m, 1H, H^3 thiophene), 8.09 (s, 1H, –N=CH), 11.16 (s, 1H, –NH–N=, D_2O exchangeable), 11.85 (s, 1H, NH pyrimidine, D_2O exchangeable). MS *m/z* [%]: 455 [$(M+2)^+$, 30], 453.1 [M^+, 100]. Anal. Calcd for $C_{25}H_{19}N_5O_2S$: C, 66.21; H, 4.22; N, 15.44. Found: C, 66.24; H, 4.27; N: 15.58.

*4.1.5. 6-Phenyl-8-(thiophen-2-yl)pyrido[2,3-d] [1,2,4]triazolo[4,3-a]pyrimidin-5(1H)-one (**6**)*

A mixture of 2-hydrazinylpyrido[2,3-*d*]pyrimidine **4** (0.34 g, 1 mmol) and triethyl orthoformate (8 mL) was heated under reflux for 3 h. The formed solid was filtered, dried and crystallized from DMF:EtOH mixture [v:v, 1:1]. Yield: 72%; m.p. > 300 °C; IR (KBr) ν: 3415 (NH), 1693 (C=O) cm^{-1}; ^1H NMR (DMSO-d_6, 300 MHz) δ: 7.26 (m, 1H, H^4 thiophene), 7.44 (m, 5H, 5 Ar–H), 7.87 (s, 1H, pyridine H), 7.91 (m, 1H, H^5 thiophene), 8.22 (m, 1H, H^3 thiophene), 9.20 (s, 1H, H^3 triazole), 12.60 (br s, 1H, NH, D_2O exchangeable); MS *m/z* [%]: 347 [$(M+2)^+$, 51.89], 345 [M^+, 66.04], 75 [100]. Anal. Calcd for $C_{18}H_{11}N_5OS$: C, 62.60; H, 3.21; N, 20.28. Found: C, 62.63; H, 3.27; N: 20.42.

*4.1.6. 6-Phenyl-8-(thiophen-2-yl)-1,2-dihydropyrido[2,3-d][1,2,4]triazolo[4,3-a]pyrimidine-3,5-dione (**7**)*

A mixture of 2-hydrazinylpyrido[2,3-*d*]pyrimidine **4** (0.34 g, 1 mmol) and ethyl chloroformate (0.22 g, 2 mmol) in dry pyridine (10 mL) was heated under reflux for 9 h. The reaction mixture was cooled and the obtained solid was filtered, washed with ethanol, dried and crystallized from DMF:EtOH [v:v, 1:1]. Yield: 86%, mp: >300 °C; IR (KBr) ν: 3371 (NH), 1687, 1651 (2C=O) cm^{-1}; ^1H NMR (DMSO-d_6, 300 MHz) δ: 7.2 (m, 1H, H^4 thiophene), 7.41 (m, 6H, 5 Ar–H + pyridine H), 7.79 (m, 1H, H^5 thiophene), 8.06 (m, 1H, H^3 thiophene), 12.23 (br s, 1H, NH, D_2O exchangeable), 12.96 (br s, 1H, NH, D_2O exchangeable); MS *m/z* [%]: 363 [$(M+2)^+$, 9.25], 361 [M^+, 36.87], 79 [100]. Anal. Calcd for $C_{18}H_{11}N_5O_2S$: C, 59.82; H, 3.07; N, 19.38. Found: C, 59.91; H, 3.05; N: 19.46.

*4.1.7. 6-Phenyl-8-(thiophen-2-yl)-3-thioxo-2,3-dihydropyrido[2,3-d][1,2,4]triazolo[4,3-a] pyrimidin-5(1H)-one (**8**)*

A mixture of 2-hydrazinylpyrido[2,3-*d*]pyrimidine **4** (0.68 g, 2 mmol), potassium hydroxide (0.23 g, 4 mmol) and carbon disulphide (4 mL) in absolute ethanol (40 mL) was heated under reflux for 5 h. The reaction mixture was evaporated to dryness and water (200 mL) was added then, the alkaline solution was filtered. The filtrate was acidified with conc. HCl (10 mL) and the separated solid was filtered, dried and crystallized from DMF:EtOH [v:v, 1:1]. Yield: 62%, m.p. > 300 °C; IR (KBr) ν: 3421 (NH), 1668 (C=O) cm^{-1}; ^1H NMR (DMSO-d_6, 300 MHz) δ: 7.17 (m, 1H, H^4 thiophene), 7.37 (m, 5H, Ar–H), 7.64 (s, 1H, pyridine H), 7.74 (m, 1H, H^5 thiophene), 8.04 (m, 1H, H^3 thiophene), 12.45 (br s, 1H, NH, D_2O exchangeable), 13.52 (br s, 1H, NH, D_2O exchangeable); MS *m/z* [%]: 379 [$(M+2)^+$, 12.7], 377 [M^+, 100]. Anal. Calcd for $C_{18}H_{11}N_5OS_2$: C, 57.28; H, 2.94; N, 18.55. Found: C, 57.34; H, 3.02; N: 18.68.

*4.1.8. 3-Amino-6-phenyl-8-(thiophen-2-yl)pyrido[2,3-d][1,2,4]triazolo[4,3-a]pyrimidin-5(1H)-one (**9**)*

A mixture of 2-hydrazinylpyrido[2,3-*d*]pyrimidine **4** (0.68 g, 2 mmol) and ammonium thiocyanate (2.38 g, 30 mmol) in glacial acetic acid (20 mL) was heated under reflux for 10 h. The reaction mixture was cooled, poured onto water (50 mL) and the formed solid was filtered, dried and crystallized from acetic acid. Yield: 68%, m.p. > 300 °C; IR (KBr) ν: 3444, 3419 (NH + NH_2), 1699 (C=O) cm^{-1}; ^1H NMR (DMSO-d_6, 300 MHz) δ: 6.9 (s, 2H, NH_2, D_2O exchangeable), 7.25 (m, 1H, H^4 thiophene), 7.44 (m, 5H, Ar–H), 7.69 (s, 1H, pyridine H), 7.87 (m, 1H, H^5 thiophene), 8.16 (m, 1H, H^3 thiophene), 12.48 (br s, 1H, NH, D_2O exchangeable); ^{13}C NMR (DMSO-d_6, 100 MHz) δ: 105.2, 108.94, 117.15, 119.88, 127.91, 128.43, 129.03, 129.61, 129.8, 132.28, 139.47, 142.95, 148.17, 153.47, 155.47, 160.18; MS *m/z* [%]: 362 [$(M+2)^+$, 6.3], 360 [M^+, 16.02], 80 [100]. Anal. Calcd for $C_{18}H_{12}N_5OS$: C, 59.99; H, 3.36; N, 23.32. Found: C, 60.08; H, 3.43; N: 23.50.

*4.1.9. 3-Methyl-6-phenyl-8-(thiophen-2-yl)pyrido[2,3-d][1,2,4] triazolo[4,3-a]pyrimidin-5(1H)-one (**10**)*

A Suspension of 2-hydrazinylpyrido[2,3-*d*]pyrimidine **4** (0.34 g, 1 mmol) and acetyl chloride (0.1 mL, 1.5 mmol) in dry pyridine (8 mL) was heated under reflux for 20 h. The reaction mixture was cooled and the formed solid was filtered, dried and crystallized from DMF:EtOH [v:v, 1:1]. Yield: 55%, m.p. > 300 °C; IR (KBr) *ν*: 3445 (NH), 1705 (C═O) cm^{-1}; ^1H NMR (DMSO-d_6, 300 MHz) *δ*: 2.95 (s, 3H, −CH_3), 7.24 (m, 1H, H^4 thiophene), 7.44 (m, 5H, Ar−H), 7.73 (s, 1H, pyridine H), 7.88 (m, 1H, H^5 thiophene), 8.15 (m, 1H, H^3 thiophene), 12.56 (br s, 1H, NH, D_2O exchangeable); MS *m/z* [%]: 361 [$(M+2)^+$, 7.68], 359 [M^+, 100]. Anal. Calcd for $C_{19}H_{13}N_5OS$: C, 63.49; H, 3.65; N, 19.49. Found: C, 63.52; H, 3.71; N: 19.62.

*4.1.10. 3-Substituted-1-(aryl)-6-phenyl-8-(thiophen-2-yl)pyrido [2,3-d][1,2,4]triazolo[4,3-a] pyrimidin-5(1H)-ones **15a**–**i***

To a mixture of 5-phenyl-7-(thiophen-2-yl)-2-thioxo-2,3-dihydropyrido[2,3-*d*] pyrimidin-4(1*H*)-one **3** (0.34 g, 1 mmol) and the appropriate hydrazonoyl chloride **11a**–**i** (1 mmol) in dioxane (50 mL), triethylamine (0.14 mL, 1 mmol) was added. The reaction mixture was refluxed for 6–10 h till the disappearance of starting materials (monitored by TLC) and hydrogen sulfide gas ceased to liberate. The solvent was removed under vacuum and the residue was triturated with methanol. The formed solid was filtered and crystallized from DMF:EtOH [v:v, 1:1].

*4.1.10.1. 3-Acetyl-1,6-diphenyl-8-(thiophen-2-yl)pyrido[2,3-d][1,2,4] triazolo[4,3-a] pyrimidin-5(1H)-one **(15a)**.* Yield: 68%; m.p.: 300 °C; IR (KBr) *ν*: 1710, 1697 (2C═O) cm^{-1}; ^1H NMR (DMSO-d_6, 300 MHz) *δ*: 2.64 (s, 3H, CO$\underline{CH_3}$), 7.23 (m, 1H, H^4 thiophene), 7.46 (m, 6H, Ar−H), 7.67–7.73 (m, 3H, 2 Ar−H + pyridine H), 7.85 (m, 1H, H^5 thiophene), 8.16 (m, 1H, H^3 thiophene), 8.23 (d, *J* = 7.5 Hz, 2H, Ar−H); MS *m/z* [%]: 464 [$(M+1)^+$, 0.43], 463 [M^+, 2.99], 73 [100]. Anal. Calcd for $C_{26}H_{17}N_5O_2S$: C, 67.37; H, 3.70; N, 15.11. Found: C, 67.35; H, 3.74; N: 15.30.

*4.1.10.2. 3-Acetyl-1-(4-fluorophenyl)-6-phenyl-8-(thiophen-2-yl) pyrido[2,3-d][1,2,4]triazolo [4,3-a] pyrimidin-5(1H)-one (**15b**).* Yield: 75%; m.p. > 300 °C; IR (KBr) *ν*: 1726, 1691 (2C═O) cm^{-1}; ^1H NMR (DMSO-d_6, 300 MHz) *δ*: 2.62 (s, 3H, CO$\underline{CH_3}$), 7.24 (m, 1H, H^4 thiophene), 7.47–7.59 (m, 7H, Ar−H), 7.73 (s, 1H, pyridine H), 7.85 (m, 1H, H^5 thiophene), 8.16 (m, 1H, H^3 thiophene), 8.21–8.24 (m, 2H, Ar−H); ^{13}C NMR (DMSO-d_6, 75 MHz) *δ*: 29.4 (CO$\underline{CH_3}$), 106.58, 116.16, 116.47, 117.03, 123.53, 127.60, 127.89, 128.19, 128.77, 128.99, 131.53, 139.22, 141.39, 143.31, 146.93, 154.26, 154.74, 156.57, 160.08, 162.44, 187.07; MS *m/z* [%]: 483 [$(M+2)^+$, 5.78], 481 [M^+, 43.72], 105 [100]. Anal. Calcd for $C_{26}H_{16}FN_5O_2S$: C, 64.86; H, 3.35; N, 14.54. Found: C, 64.92; H, 3.37; N: 14.72%.

*4.1.10.3. 3-Acetyl-1-(4-chlorophenyl)-6-phenyl-8-(thiophen-2-yl) pyrido[2,3-d][1,2,4]triazolo [4,3-a]pyrimidin-5(1H)-one (**15c**).* Yield: 71%; m.p. > 300 °C; IR (KBr) *ν*: br, 1676 (2C═O) cm^{-1}; ^1H NMR (DMSO-d_6, 300 MHz) *δ*: 2.65 (s, 3H, CO$\underline{CH_3}$), 7.24 (m, 1H, H^4 thiophene), 7.45 (m, 5H, Ar−H), 7.71 (s, 1H, pyridine H), 7.73 (d, *J* = 6.9 Hz, 2H, Ar−H), 7.85 (m, 1H, H^5 thiophene), 8.13 (m, 1H, H_3 thiophene), 8.27 (d, *J* = 6.9 Hz, 2H, Ar−H); MS *m/z* [%]: 499 [$(M+2)^+$, 41.24], 497 [M^+, 100]. Anal. Calcd for $C_{26}H_{16}ClN_5O_2S$: C, 62.71; H, 3.24; N, 14.06. Found: C, 62.76; H, 3.27; N: 14.15.

*4.1.10.4. 3-Acetyl-6-phenyl-8-(thiophen-2-yl)-1-p-tolylpyrido[2,3-d] [1,2,4]triazolo[4,3-a]pyrimidin-5(1H)-one (**15d**).* Yield: 70%; m.p. > 300 °C; IR (KBr) *ν*: 1715, 1697 (C═O) cm^{-1}; ^1H NMR (DMSO-d_6, 300 MHz) *δ*: 2.43 (s, 3H, CH_3), 2.64 (s, 3H, CO$\underline{CH_3}$), 7.24 (m, 1H, H^4 thiophene), 7.47 (m, 7H, Ar−H), 7.72 (s, 1H, pyridine H), 7.86 (m, 1H, H^5 thiophene), 8.07 (d, *J* = 8.4 Hz, 2H, Ar−H), 8.16 (m, 1H, H^3 thiophene); MS *m/z* [%]: 479 [$(M+2)^+$, 10.19], 477 [M^+, 100]. Anal. Calcd for $C_{27}H_{19}N_5O_2S$: C, 67.91; H, 4.01; N, 14.67. Found: C, 67.98; H, 3.97; N: 14.79.

*4.1.10.5. 3-Acetyl-1-(4-methoxyphenyl)-6-phenyl-8-(thiophen-2-yl) pyrido[2,3-d][1,2,4]triazolo[4,3-a]pyrimidin-5(1H)-one (**15e**).* Yield: 75%; m.p. > 300 °C; IR (KBr) *ν*: 1728, 1695 (2C═O) cm^{-1}; ^1H NMR (DMSO-d_6, 300 MHz) *δ*: 2.65 (s, 3H, CO$\underline{CH_3}$), 3.31 (s, 3H, OCH_3), 7.25 (m, 1H, H^4 thiophene), 7.45 (m, 5H, Ar−H), 7.74 (s, 1H, pyridine H), 7.77 (d, *J* = 6.9 Hz, 2H, Ar−H), 7.86 (m, 1H, H^5 thiophene), 8.17 (m, 1H, H^3 thiophene), 8.27 (d, *J* = 6.9 Hz, 2H, Ar−H); MS *m/z* [%]: 493 [M^+, 60], 66 [100]. Anal. Calcd for $C_{27}H_{19}N_5O_3S$: C, 65.71; H, 3.88; N, 14.19. Found: C, 65.74; H, 3.93; N: 14.32.

*4.1.10.6. 4-(3-Acetyl-5-oxo-6-phenyl-8-(thiophen-2-yl)pyrido[2,3-d] [1,2,4]triazolo[4,3-a] pyrimidin-1(5H)-yl)benzenesulfonamide (**15f**).* Yield: 65%; m.p. > 300 °C; IR (KBr) *ν*: 3402, 3358 (NH_2), br, 1710 (2C═O), 1348, 1166 (SO_2) cm^{-1}; ^1H NMR (DMSO-d_6, 300 MHz) *δ*: 2.88 (s, 3H, $COCH_3$), 7.25 (m, 1H, H^4 thiophene), 7.47–7.48 (m, 5H, Ar−H), 7.53 (br.s, 2H, NH_2, D_2O exchangeable), 7.77 (s, 1H, pyridine H), 7.88 (m, 1H, H^5 thiophene), 8.13 (d, *J* = 8.7 Hz, 2H, Ar−H), 8.16 (m, 1H, H^3 thiophene), 8.46 (d, *J* = 8.7 Hz, 2H, Ar−H); ^{13}C NMR (DMSO-d_6, 75 MHz) *δ*: 29.38 (CO$\underline{CH_3}$), 106.78, 117.28, 120.67, 127.06, 127.69, 128.06, 128.16, 128.97, 129.08, 131.66, 138.69, 138.92, 141.65, 142.01, 142.92, 146.84, 154.32, 154.59, 156.51, 159.82, 162.62, 187.37; MS *m/z* [%]: 543 [$(M+1)^+$, 0.46], 542 [M^+, 0.47], 73.05 [100]. Anal. Calcd for $C_{26}H_{18}N_6O_4S_2$: C, 57.55; H, 3.34; N, 15.49. Found: C, 57.54; H, 3.42; N: 15.63.

*4.1.10.7. Ethyl 5-oxo-1,6-diphenyl-8-(thiophen-2-yl)-1,5-dihydropyrido[2,3-d][1,2,4]triazolo[4,3-a]pyrimidine-3-carboxylate (**15g**).* Yield: 70%; m.p. 290–292 °C; IR (KBr) *ν*: 1749, 1705 (2C═O) cm^{-1}; ^1H NMR (DMSO-d_6, 300 MHz) *δ*: 1.30 (t, *J* = 6.9 Hz, 3H, $CH_2\underline{CH_3}$), 4.43 (q, *J* = 6.9 Hz, 2H, $\underline{CH_2}CH_3$), 7.24 (m, 1H, H^4 thiophene), 7.46–7.52 (m, 6H, Ar−H), 7.66–7.71 (m, 2H, Ar−H), 7.73 (s, 1H, pyridine H), 7.85 (m, 1H, H^5 thiophene), 8.15–8.18 (m, 3H, 2 Ar−H + H^3 thiophene); MS *m/z* [%]: 495 [$(M+2)^+$, 3.44], 493 [M^+, 39.34], 71.05 [100]. Anal. Calcd for $C_{27}H_{19}N_5O_3S$: C, 65.71; H, 3.88; N, 14.19. Found: C, 65.74; H, 3.90; N: 14.35. The purified product **15g** was dissolved in ethanol/DMF (v/v = 3/1) and yellow single crystals were separated after 3 days. Crystal data for compound **15g**: Molecular formula $C_{27}H_{19}N_5O_3S$, Formula weight: 493.54, Orthorhombic, *Pbca*, a = 19.6064 (6) Å, b = 10.9685 (4) Å, c = 21.7093 (8) Å, V = 4668.7 (3) $Å^3$, D_{calc} = 1.404 Mg m^{-3}, colorless block with 0.32 × 0.19 × 0.15 mm. A total of 29344 reflections were measured, of which 3939 were independent. R_{int} = 0.078, Dataset (h; k; l) = −23,23; −12,12; −23,25. Refinement of F^2, against all reflections, led to R [$F^2 > 2\sigma(F^2)$] = 0.090, $wR(F^2)$ = 0.296, S = 1.06.

*4.1.10.8. Ethyl1-(4-chlorophenyl)-5-oxo-6-phenyl-8-(thiophen-2-yl)-1,5-dihydropyrido[2,3-d] [1,2,4] triazolo[4,3-a]pyrimidine-3-carboxylate (**15h**).* Yield: 75%; m.p. > 300 °C; IR (KBr) *ν*: 1743, 1699 (2C═O) cm^{-1}; ^1H NMR (DMSO-d_6, 300 MHz) *δ*: 1.3 (t, *J* = 7.5 Hz, 3H, $CH_2\underline{CH_3}$), 4.42 (q, *J* = 7.5 Hz, 2H, $\underline{CH_2}CH_3$), 7.23 (m, 1H, H^4 thiophene), 7.45 (m, 5H, Ar−H), 7.74 (s, 1H, pyridine H), 7.75 (d, *J* = 8.7 Hz, 2H, Ar−H), 7.86 (m, 1H, H^5 thiophene), 8.18 (m, 1H, H^3 thiophene), 8.22 (d, *J* = 8.7 Hz, 2H, Ar−H); ^{13}C NMR (DMSO-d_6, 75 MHz) *δ*: 13.61($CH_2\underline{CH_3}$), 63.42 ($\underline{CH_2}CH_3$), 106.48, 117.09, 122.45, 127.61, 127.97, 128.23, 128.81, 129.09, 129.44, 131.59, 131.66, 135.13, 135.57, 139.07, 143.27, 146.5, 154.13, 154.44, 156.07, 156.60, 160.06; MS *m/z* [%]: 529 [$(M+2)^+$, 1.38], 527 [M^+, 3.85], 80 [100]. Anal. Calcd for $C_{27}H_{18}ClN_5O_3S$: C, 61.42; H, 3.44; N, 13.26. Found: C, 61.48; H, 3.42; N: 13.39.

*4.1.10.9. Ethyl 5-oxo-6-phenyl-8-(thiophen-2-yl)-1-p-tolyl-1,5-dihydropyrido[2,3-d][1,2,4] triazolo[4,3-a]pyrimidine-3-carboxylate (**15i**).* Yield: 68%; m.p. 283–285 °C; IR (KBr) ν: 1755, 1716 (2C=O) cm^{-1}; ^1H NMR (DMSO-d_6, 300 MHz) δ: 1.3 (t, J = 6.9 Hz, 3H, $CH_2\underline{CH_3}$), 2.43 (s, 3H, CH_3), 4.42 (q, J = 6.9 Hz, 2H, $\underline{CH_2}CH_3$), 7.24 (m, 1H, H^4 thiophene), 7.46–7.50 (m, 7H, Ar–H), 7.71 (s, 1H, pyridine H), 7.86 (m, 1H, H^5 thiophene), 8.03 (d, J = 8.1 Hz, 2H, Ar–H), 8.16 (m, 1H, H^3 thiophene); ^{13}C NMR (DMSO-d_6, 75 MHz) δ: 13.62($CH_2\underline{CH_3}$), 20.6 (CH_3), 63.32 ($\underline{CH_2}CH_3$), 106.3, 116.84, 121.27, 127.59, 127.93, 128.24, 128.79, 128.98, 129.77, 131.55, 133.82, 135.23, 137.22, 139.17, 143.38, 146.53, 154.11, 154.53, 156.19, 156.53, 160.22; MS m/z [%]: 508 [$(M+1)^+$, 1.25], 507 [M^+,5.26], 73[100]. Anal. Calcd for $C_{28}H_{21}N_5O_3S$: C, 66.26; H, 4.17; N, 13.80. Found: C, 66.34; H, 4.21; N: 13.96.

*4.1.10.10. Ethyl 5-oxo-6-phenyl-1-(4-sulfamoylphenyl)-8-(thiophen-2-yl)-1,5-dihydropyrido[2,3-d][1,2,4]triazolo[4,3-a]pyrimidine-3-carboxylate (**15j**).* Yield: 71%; m.p. > 300 °C; IR (KBr) ν: 3325, 3286 (NH_2), br, 1737,1707 (2C=O), 1346, 1159 (SO_2) cm^{-1}; ^1H NMR (DMSO-d_6, 400 MHz) δ: 1.31 (t, J = 7.12 Hz, 3H, $CH_2\underline{CH_3}$), 4.44 (q, J = 7.12 Hz, 2H, $\underline{CH_2}CH_3$), 7.25 (t, J = 4.64 Hz, 1H, H^4 thiophene), 7.43–7.48 (m, 5H, Ar–H),7.53 (br.s, 2H, NH_2, D_2O exchangeable), 7.77 (s, 1H, pyridine H), 7.87 (d, J = 4.92 Hz, 1H, H^5 thiophene), 8.12 (d, J = 8.76 Hz, 2H, Ar–H), 8.19 (d, J = 3.68 Hz, 1H, H^3 thiophene), 8.43 (d, J = 8.76 Hz, 2H, Ar–H). ^{13}C NMR (DMSO-d_6, 100 MHz) δ: 13.74 ($CH_2\underline{CH_3}$), 63.40 ($\underline{CH_2}CH_3$), 106.4, 116.87, 117.04, 121.11, 127.64, 128.16, 128.78, 129.10, 129.49, 131.64, 131.77, 135.38, 136.25, 139.16, 143.37, 146.59, 154.1, 154.57, 156.23, 156.55, 160.19. Anal. Calcd for $C_{27}H_{20}N_6O_5S_2$: C, 56.63; H, 3.52; N, 14.68; O, 13.97; S, 11.20. Found: C, 56.42; H, 3.43; N: 14.86.

4.2. Biological evaluation

4.2.1. In vitro cytotoxic activity [28]

A-549 human lung cancer cells and PC-3 human prostate cancer cells were grown in DMEM and RPMI-1640 respectively. Both were supplemented with 10% heat inactivated FBS, 50 units/mL of penicillin and 50 g/mL of streptomycin and maintained at 37 °C in a humidified atmosphere containing 5% CO_2. The cells were maintained as "monolayer culture" by serial subculturing. Cytotoxicity was determined using SRB method as previously described by Skehan et al. [28]. Exponentially growing cells were collected using 0.25% Trypsin-EDTA and seeded in 96-well plates at 1000–2000 cells/well in DMEM supplemented medium. After 24 h, cells were incubated for 48 h with various concentrations of the tested compounds as well as 5-fluorouracil as reference compound. Following 48 h of treatment, the cells will be fixed with 10% trichloroacetic acid for 1 h at 4 °C. Wells were stained for 10 min at room temperature with 0.4% SRB dissolved in 1% acetic acid. The plates were air dried for 24 h and the dye was solubilized with Tris–HCl for 5 min on a shaker at 1600 rpm. The optical density (OD) of each well was measured spectrophotometrically at 564 nm with an ELISA microplate reader (ChroMate-4300, FL, USA). The IC_{50} values were calculated according to the equation for Boltzmann sigmoidal concentration–response curve using the nonlinear regression fitting models (Graph Pad, Prism Version 5). The results reported are means of at least three separate experiments. Significant differences were analyzed according by way ANOVA wherein the differences were considered to be significant at $p < 0.05$.

4.2.2. Morphological investigation

PC-3 cells were cultured in cell culture flask 25 cm^2 (3×10^6 cells/flask) and treated with a fixed concentration IC_{50} (0.356 μM) of the tested compound **15f** for 24 or 48 h. Then the cells were stained using the nucleic acid-binding dye mixture of 100 μg/mL acridine orange and 100 μg/mL ethidium bromide in PBS, and examined by fluorescence microscopy.

4.2.3. Caspase-3 activity determination

The level of caspase-3 was measured using the colorimetric assay kit (Uscn Life Science E90626Mu, China) according to the manufacturer's instructions. Briefly, PC-3 cells were treated with **15f** (0.356 μM) for 24 or 48 h. The cell were harvested by trypsinization and rinsed with PBS. After centrifugation, the pellet (10^5–10^6 cells) was suspended in 1 mL of PBS. Cells were freezed at <−20 °C and thawed with gentle mixing. Freeze/thaw cycle repeated for 3 times, then centrifuged at 1500 × g for 10 min at 2–8 °C to remove cellular debris.

The test principle applied in this kit is sandwich enzyme immunoassay. The microtiter plate provided in this kit has been pre-coated with an antibody specific to active caspase-3. The cell lysates were then added to the appropriate microtiter plate wells with a biotin-conjugated antibody specific to caspase-3. Next, Avidin conjugated to Horseradish Peroxidase (HRP) is added to each microplate well and incubated. After TMB substrate solution is added, only those wells that contain caspase-3, biotin-conjugated antibody and enzyme-conjugated Avidin will exhibit a change in color. The enzyme–substrate reaction is terminated by the addition of sulfuric acid solution and the color change is measured spectrophotometrically at a wavelength of 450 nm ± 10 nm. The concentration of caspase-3 in the samples is then determined in ng/g protein.

4.2.4. Cell cycle analysis

The PC-3 cells were treated with 0.356 μM of **15f** for 24 or 48 h. After treatment, the cells were washed twice with ice-cold PBS, collected by centrifugation, and fixed in ice-cold 70% (v/v) ethanol, washed with PBS, re-suspended with 0.1 mg/mL RNase, stained with 40 mg/mL PI, and analyzed by flow cytometry using FACScalibur (Becton Dickinson). The cell cycle distributions were calculated using Cell Quest software (Becton Dickinson).

4.2.5. CDK4/Cyclin D1 and CDK6/Cyclin D1profiling

A radioisotope assay format was used for profiling evaluation of protein kinase targets and all assays are performed in a designated radioactive working area. Protein kinase assays (in duplicate) were performed at ambient temperature for 20–30 min in a final volume of 25 μL according to [5 μL of diluted active CDK4/Cyclin D1 or CDK6/Cyclin D (~10–50 nM final concentration in the assay)], 5 μL of stock solution of substrate (1–5 μg of peptide substrate), 5 μL of kinase assay buffer, 5 μL of compound (various concentration) or 10% DMSO and 5 μL of ^{33}P-ATP (250 μM stock solution, 0.8 μCi).

The assay was initiated by the addition of ^{33}P-ATP and the reaction mixture was incubated at ambient temperature for 20–30 min. After the incubation period, the assay was terminated by spotting 10 μL of the reaction mixture onto Multiscreen phosphocellulose P81 plate. The Multiscreen phosphocellulose P81 plate was washed 3 times for approximately 15 min each in a 1% phosphoric acid solution. The radioactivity on the P81 plate was counted in the presence of scintillation fluid in a Trilux scintillation counter.

Blank control was set up that included all the assay components except the addition of the appropriate substrate (replaced with equal volume of assay dilution buffer). The corrected activity for CDK4/Cyclin D1 and CDK6/Cyclin D1 was determined by subtracting the blank control value.

4.2.6. Immunocytochemistry staining for p21 and p27 [45]

PC-3 cells were seeded on ibidi® μ-Chamber 12-well slide (Munich, Germany) at a density of 2 × 10^5 cells/mL. After exposure

to the tested compound **15f** at a concentration equivalent to its IC_{50} (0.36 μM) for 48 h, cells were fixed with 70% of ethanol. Then, they were washed in phosphate-buffered saline (PBS) and incubated with 0.01% Triton X-100 in PBS for 1 min to permeabilize the cell membranes. Cells were afterward incubated with 0.3% of H_2O_2 in PBS for 20 min to quench endogenous peroxidase activity and then in 5% of normal horse serum in Tris-buffered saline plus Tween-20 (TBST) for 30 min to block the nonspecific binding of the secondary antibody. Thereafter, cells were incubated overnight with primary anti-p21 antibody or anti-p27 antibody (Abcam plc, Cambridge, MA). In the following day, the slides were incubated with the corresponding conjugated anti-rabbit IgG (dilution, 1:2,000, Santa Cruz Biotechnology, Dallas, TX). Cells were treated afterward with streptavidin horseradish peroxidase complex (dilution, 1:100; ABC/HRP; Vector Laboratories, Burlingame, CA, USA) in TBST for 50 min. The color reaction was developed for 5 min in 3,30-diaminobenzidine (DAB) solution (Santa Cruz Biotechnology, Dallas, TX).

4.2.7. *Western blot analysis [45]*

PC-3 cells were seeded, cultured and exposed to IC_{50} of the tested compound **15f** (0.36 μM) for 48 h. Whole-cell protein lysates were prepared according to standard protocol using RIPA buffer (Cell Signaling, Danvers, MA). Protein (50 mg) was loaded per well of a 10% SDS-PAGE gel using electrophoresis buffer (0.192 M glycine, 25 mM Tris and 0.1% SDS). After electrophoresis, the gel was transferred onto a PVDF membrane (Bio-Rad Laboratories, Hercules, CA) using transfer buffer (0.192 M glycine, 25 mM Tris, 0.025% SDS and 10% methanol). Membranes were blocked in TBS-T with 5% BSA and incubated overnight with the primary antibody anti-p21 antibody (1:1000; Abcam plc, Cambridge, MA) then incubated with secondary HRP-linked antibody (1:5000). Development was done using Pierce ECL 2 chemiluminescent and chemifluorescent substrate (Thermo Fisher Scientific, Waltham, MA). Anti-β-tubulin antibody (Abcam plc, Cambridge, MA) was used for loading correction. Band densities were quantified using the free software "ImageJ".

Acknowledgments

Pharmaceutical Chemistry Department, Faculty of Pharmacy, Cairo University, Egypt, is highly appreciated for funding this research work, and for X-ray research, the authors would like to extend their sincere appreciation to the Deanship of Scientific Research at King Saud University for its funding of this research through the Research Group Project no. RGP-VPP-321.

Appendix A. Supplementary data

Supplementary data related to this article can be found at http://dx.doi.org/10.1016/j.ejmech.2014.06.027.

References

[1] A. Kamal, D. Dastagiri, M.J. Ramaiah, J.S. Reddy, E.V. Bharathi, M.K. Reddy, M.V. Sagar, T.L. Reddy, S.N. Pushpavalli, M. Pal-Bhadra, Eur. J. Med. Chem. 46 (2011) 5817–5824.
[2] L.W. Zheng, Y. Li, D. Ge, B.X. Zhao, Y.R. Liu, H.S. Lv, J. Ding, J.Y. Miao, Bioorg. Med. Chem. Lett. 20 (2010) 4766–4770.
[3] I. Vermes, C. Haanen, C. Reutelingsperger, J. Immunol. Methods 243 (2000) 167–190.
[4] S.X. Cai, B. Nguyen, S. Jia, J. Herich, J. Guastella, S. Reddy, B. Tseng, J. Drewe, S. Kasibhatla, J. Med. Chem. 46 (2003) 2474–2481.
[5] L. Cordeu, E. Cubedo, E. Bandres, A. Rebollo, X. Saenz, H. Chozas, M. Victoria Dominguez, M. Echeverria, B. Mendivil, C. Sanmartin, J.A. Palop, M. Font, J. Garcia-Foncillas, Bioorg. Med. Chem. 15 (2007) 1659–1669.
[6] S. Wang, Q. Wang, Y. Wang, L. Liu, X. Weng, G. Li, X. Zhang, X. Zhou, Bioorg. Med. Chem. Lett. 18 (2008) 6505–6508.
[7] H.Z. Zhang, S. Kasibhatla, J. Kuemmerle, W. Kemnitzer, K. Ollis-Mason, L. Qiu, C. Crogan-Grundy, B. Tseng, J. Drewe, S.X. Cai, J. Med. Chem. 48 (2005) 5215–5223.
[8] P.L. Toogood, P.J. Harvey, J.T. Repine, D.J. Sheehan, S.N. VanderWel, H. Zhou, P.R. Keller, D.J. McNamara, D. Sherry, T. Zhu, J. Brodfuehrer, C. Choi, M.R. Barvian, D.W. Fry, J. Med. Chem. 48 (2005) 2388–2406.
[9] S.N. VanderWel, P.J. Harvey, D.J. McNamara, J.T. Repine, P.R. Keller, J. Quin 3rd, R.J. Booth, W.L. Elliott, E.M. Dobrusin, D.W. Fry, P.L. Toogood, J. Med. Chem. 48 (2005) 2371–2387.
[10] B.D. Palmer, J.B. Smaill, G.W. Rewcastle, E.M. Dobrusin, A. Kraker, C.W. Moore, R.W. Steinkampf, W.A. Denny, Bioorg. Med. Chem. Lett. 15 (2005) 1931–1935.
[11] K. Malagu, H. Duggan, K. Menear, M. Hummersone, S. Gomez, C. Bailey, P. Edwards, J. Drzewiecki, F. Leroux, M.J. Quesada, G. Hermann, S. Maine, C.A. Molyneaux, A. Le Gall, J. Pullen, I. Hickson, L. Smith, S. Maguire, N. Martin, G. Smith, M. Pass, Bioorg. Med. Chem. Lett. 19 (2009) 5950–5953.
[12] C. Sanmartin, M.V. Dominguez, L. Cordeu, E. Cubedo, J. Garcia-Foncillas, M. Font, J.A. Palop, Arch. Pharm. 341 (2008) 28–41.
[13] M. Font, A. Gonzalez, J.A. Palop, C. Sanmartin, Eur. J. Med. Chem. 46 (2011) 3887–3899.
[14] J.F. Dorsey, R. Jove, A.J. Kraker, J. Wu, Cancer Res. 60 (2000) 3127–3131.
[15] G.S. Hassan, H.H. Kadry, S.M. Abou-Seri, M.M. Ali, A.E. Mahmoud, Bioorg. Med. Chem. 19 (2011) 6808–6817.
[16] L.W. Zheng, L.L. Wu, B.X. Zhao, W.L. Dong, J.Y. Miao, Bioorg. Med. Chem. 17 (2009) 1957–1962.
[17] S. Rollas, Ş.G. Küçükgüzel, Molecules 12 (2007) 1910–1939.
[18] H.N. Hafez, A.R. El-Gazzar, Bioorg. Med. Chem. Lett. 19 (2009) 4143–4147.
[19] X.L. Zhao, Y.F. Zhao, S.C. Guo, H.S. Song, D. Wang, P. Gong, Molecules 12 (2007) 1136–1146.
[20] A.S. Shawali, S.M. Sherif, M.A. Darwish, M.M. El-merzabani, Arch. Pharmacal Res. 33 (2010) 55–60.
[21] S. Wawzonek, J. Org. Chem. 41 (1976) 310–313.
[22] J.R.G.W. Davey, J. Chem. Soc. (1953) 1008–1014.
[23] B.I. J.Quiroga, A. Sanchez, M. Nogueras, H. Meier, J. Het. Chem. 29 (1992) 1045.
[24] J. Reiter, L. Bongo, P. Dyortsok, Tetrahedron Lett. 43 (1987) 2497–2504.
[25] H.M.E. Hassaneen, ARKIVOC (2007) 154–163.
[26] A.-R.B.A. El-Gazzar, M.M. El-Enany, M.N. Mahmoud, Bioorg. Med. Chem. 16 (2008) 3261–3273.
[27] H.M. Hassneen, T.A. Abdallah, Molecules 8 (2003) 333–341.
[28] P. Skehan, R. Storeng, D. Scudiero, A. Monks, J. McMahon, D. Vistica, et al., J. Natl. Cancer Inst. 82 (1990) 1107–1112.
[29] F.J. Zhao, S. Zhang, Z.M. Yu, S.J. Xia, H. Li, Prostate Cancer P. D. 12 (2009) 166–171.
[30] D. Longley, D. Harkin, P. Johnston, Nat. Rev. Cancer 3 (2003) 330–338.
[31] K. Fukuoka, J. Usuda, Y. Iwamoto, H. Fukumoto, T. Nakamura, T. Yoneda, N. Narita, N. Saijo, K. Nishio, Investig. New Drugs 19 (2001) 219–227.
[32] C.T. Supuran, World J. Clin. Oncol. 3 (2012) 98–103.
[33] F. Carta, A. Scozzafava, C.T. Supuran, Sulfonamides: a patent review (2008–2012), Expert Opin. Ther. Pat. 22 (2012) 747–758.
[34] W.O. Foye, T.L. Lemke, D.A. Williams, Foye's Principles of Medicinal Chemistry, sixth ed., Wolters Kluwer/Lippincott Williams & Wilkins, Philadelphia, 2008, p. 285 (Chapter 10).
[35] R. Ikeda, T. Iwaki, T. Iida, T. Okabayashi, E. Nishi, M. Kurosawa, N. Sakai, T. Konakahara, Eur. J. Med. Chem. 46 (2011) 636–646.
[36] C. Lou, M. Wang, G. Yang, H. Cai, Y. Li, F. Zhao, H. Yang, L. Tong, B. Cai, Toxicol. in vitro 23 (2009) 906–910.
[37] Y. Zhang, L. Jin, H. Xiang, J. Wu, P. Wang, D. Hu, W. Xue, S. Yang, Eur. J. Med. Chem. 66 (2013) 335–344.
[38] N.A. Thornberry, Chem. Biol. 5 (1998) 97–103.
[39] K.B. Huang, Z.F. Chen, Y.C. Liu, Z.Q. Li, J.H. Wei, M. Wang, G.H. Zhang, H. Liang, Eur. J. Med. Chem. 63 (2013) 76–84.
[40] C. Avendaño, J.C. Menéndez, Medicinal chemistry of anticancer Drugs, ScienceDirect (Online Service), Elsevier, Amsterdam; Boston, 2008, p. 275.
[41] P.L. Toogood, Med. Res. Rev. 21 (2001) 487–498.
[42] J.J. Johnson, S.M. Petiwala, D.N. Syed, J.T. Rasmussen, V.M. Adhami, I.A. Siddiqui, A.M. Kohl, H. Mukhtar, Carcinogenesis 33 (2012) 413–419.
[43] A.L. Gartel, S.K. Radhakrishnan, Cancer Res. 65 (2005) 3980–3985.
[44] R. Rodriguez, M. Meuth, Mol. Biol. Cell. 17 (2006) 402–412.
[45] M.F. Tolba, A. Esmat, A.M. Al-Abd, S.S. Azab, A.E. Khalifa, H.A. Mosli, Abdel-S.Z. Rahman, A.B. Abdel-Naim, IUBMB Life 65 (2013) 716–729.